

Half-shell $\alpha + \alpha$ scattering

L. P. Kok

*Institute for Theoretical Physics, Groningen, The Netherlands
and Department of Physics and Astronomy, University of Maryland, College Park, Maryland 20742*

J. E. Holwerda and J. W. de Maag

Institute for Theoretical Physics, Groningen, The Netherlands

(Received 27 September 1982)

For a given $\alpha\alpha$ potential we show how to calculate in a convenient way the half-off-the-energy-shell cross section σ_{half} for $\alpha\alpha$ scattering. We compute σ_{half} numerically for energies up to 125 MeV (lab), and make a comparison with the free-scattering cross section. Coulomb effects are included rigorously. In particular, we recall that σ_{half} is a discontinuous function of the off-shell-momentum variable at the on-shell value. We confirm that off-shell effects are sizeable, and discuss the relevance for the plane-wave impulse approximation and distorted-wave impulse approximation descriptions of $(\alpha, 2\alpha)$ reactions.

[NUCLEAR REACTIONS Half-shell scattering, Coulomb potential, im-
pulse approximations, $\alpha + \alpha$ system.]

I. INTRODUCTION

Knock-out reactions have been highly successful in the study of particle distributions in nuclei. Recently reactions such as $(p, p\alpha)$ and $(\alpha, 2\alpha)$ have been used to extract information about α clustering in nuclei. The analysis of the experimental data for these processes is commonly done with the plane-wave impulse approximation (PWIA) or the distorted-wave impulse approximation (DWIA). In these procedures the cross section has a factorized form. Schematically, the following factors occur:

$$\frac{d^3\sigma}{d\Omega_x d\Omega_\alpha dE} = N_{\text{eff}}(\text{PSF})(\text{MD}) \frac{d\sigma}{d\Omega_{x\alpha}}(E_{x\alpha}, \theta_{x\alpha}). \quad (1.1)$$

The phase-space factor (PSF) contains known kinematical forms, whereas (MD) is a (possibly distorted) momentum distribution which harbors the α clustering information. Furthermore, $d\sigma/d\Omega_{x\alpha}$ is the two-body cross section for the $x + \alpha$ scattering process, where x is the projectile. Finally, N_{eff} is an effective normalization constant which often has to be invoked in order to reconcile experiment and theory.

We refer to a recent review¹ for a full account of recent experiments and their implications in connection with the structure of nuclei (clustering) and the understanding of the reaction mechanisms. In PWIA $d\sigma/d\Omega_{x\alpha}$ is the half-off-the-energy-shell (or

briefly the half-shell) cross section for the $x + \alpha$ scattering process. It has been shown by Redish² that, even with distorted waves, the structure of the cross section given by Eq. (1.1) is correct, and that the half-shell two-body cross section can be justifiably used. A common additional approximation is to replace $d\sigma/d\Omega_{x\alpha}$ by the free (i.e., the on-shell) cross section for $x + \alpha$ scattering.

In the case of $\alpha + \alpha$ scattering the latter approximation was investigated recently by Sharma and Jain³ for incident energies from 60 to 140 MeV (lab). These authors conclude that the half-shell effects for this case are large. In their computations the effects of the Coulomb potential acting between the α particles have been neglected, or incorporated only approximately.

It is the purpose of the present paper to show how to calculate from a given realistic phenomenological $\alpha\alpha$ potential the on-shell cross section and the half-shell cross section. For various values of the energy, momentum, and angle variables we compute the cross sections. We confirm the conclusions of Ref. 3 that half-shell effects are important. Moreover, we find that the role of the Coulomb potential is important.

In Sec. II we give the formalism. Starting from a given $\alpha\alpha$ potential we give closed formulas for the cross sections. In Sec. III we specify the $\alpha\alpha$ -potential parameters. Section IV gives the results of numerical computations. Section V concludes this paper with a discussion.

II. FORMALISM

The long range of the Coulomb potential V_c is a source of special difficulties. The r^{-1} behavior of the potential between charged particles (for $r \rightarrow \infty$) causes the physical half-shell and the off-shell T matrices to have (branch-point) singularities at the on-shell value of the half-shell and off-shell momentum variables, respectively. We adopt notations and conventions developed and used previously.^{4,5} A convenient framework is provided by the so-called (Coulombian) asymptotic states $|\vec{k}_\infty \pm\rangle$. Often we suppress the $+$ symbol in this notation. In this paper we consider scattering by the $\alpha\alpha$ potential $V = V_c + V_s$. Here V_s is a spherically symmetric potential with a short-range character. The T operator can be split into the pure Coulomb T operator T_c and a remainder T_{cs} , $T = T_c + T_{cs}$. The on-shell and half-shell scattering amplitudes are connected to the physical on-shell T matrix ($k = k'$) and the physical half-shell T matrix through^{4,5}

$$f_{\text{on}}(\hat{k} \cdot \hat{k}') = -2\pi^2 \langle \vec{k}'_\infty - | T | \vec{k}_\infty \rangle, \quad \hat{k}' \neq \hat{k}, \quad k' = k \in R^+, \quad (2.1)$$

$$f_{\text{half}} = -2\pi^2 \langle \vec{p} | T | \vec{k}_\infty \rangle, \quad p \neq k, \quad (2.2)$$

$$-(2\pi^2)^{-1} f_{\text{half}}^c = \langle \vec{p} | T_c | \vec{k}_\infty \rangle = \frac{k\gamma}{\pi^2} \frac{C_0 e^{i\sigma_0}}{q^{2+2i\gamma}} \lim_{\epsilon \downarrow 0} [p^2 - (k + i\epsilon)^2]^{i\gamma}, \quad (2.4)$$

where $\hat{p} = \hat{k}'$, $p \neq k$, $\hat{p} \cdot \hat{k} = \cos\theta$, $\vec{q} = \vec{p} - \vec{k}$ is the momentum transfer,

$$|p - k| < q \leq p + k,$$

and

$$C_0^2 = 2\pi\gamma / (e^{2\pi\gamma} - 1)$$

is the Coulomb penetrability factor.

As was stressed in Ref. 6, the on-shell limits for $p \downarrow k$ and $p \uparrow k$ of the (pure Coulomb) physical half-shell Coulomb T matrix are not equal to the physical on-shell Coulomb T matrix. Both these limits do not exist. However, the on-shell limits for $p \downarrow k$ and $p \uparrow k$ of the modulus of the half-shell Coulomb T matrix do exist. These two limits differ from the modulus of the on-shell Coulomb T matrix, according to

$$\lim_{p \downarrow k} \sigma_{\text{half}} = e^{-2\pi\gamma} \lim_{p \uparrow k} \sigma_{\text{half}} = C_0^2 \sigma_{\text{on}}. \quad (2.5)$$

This relation holds not only for the pure Coulomb potential. It also holds⁶ for potentials of the type $V_c + V_s$. If the Coulomb potential is switched off (i.e., $\gamma \rightarrow 0$), then $e^{-2\pi\gamma} \rightarrow 1$ and $C_0^2 \rightarrow 1$, and σ_{half} be-

respectively. The argument E of the T operator $T(E)$, where E is the complex-valued variable, is given by $(k + i\epsilon)^2$, $\epsilon \downarrow 0$. In our notation it is often suppressed. Note that we use units such that $\hbar = 1$ and $2m = 1$, where m is the reduced mass. Usually we suppress $+i\epsilon$, and write k for $k + i\epsilon$, $\epsilon \downarrow 0$. Amplitudes and cross sections are related through $\sigma(x) = |f|^2$, where $\sigma(x)$ is a shorthand notation for $d\sigma/d\Omega$, and x stands for the cosine of the scattering angle θ in the center-of-mass system.

For pure Coulomb scattering (i.e., $V_s = 0$) the physical on-shell T matrix is given by

$$-(2\pi^2)^{-1} f_{\text{on}}^c = \langle \vec{k}'_\infty - | T_c | \vec{k}_\infty \rangle = \frac{k\gamma}{\pi^2 Q^2} e^{2i\sigma_0} \left[\frac{4k^2}{Q^2} \right]^{i\gamma}, \quad (2.3)$$

where $\hat{k}' \neq \hat{k}$, $k' = k$, $\hat{k}' \cdot \hat{k} = \cos\theta$, $\vec{Q} = \vec{k}' - \vec{k}$ is the momentum transfer, $0 < Q \leq 2k$, $\sigma_l = \arg\Gamma(l + 1 + i\gamma)$ is the Coulomb phase shift, and γ is Sommerfeld's parameter. In Eq. (2.3) f_{on}^c is the Coulomb scattering amplitude (also referred to as the Rutherford amplitude). The physical half-shell T matrix in this case is given by

comes a continuous function of the half-shell variable p in the on-shell value k .

The T operator $T_{cs}(k^2)$ is of a short-range character. The T_{cs} -matrix elements have a rapidly converging partial-wave (p.w.) series expansion, with p.w. coefficients given by the p.w. T operators $T_{csl}(k^2)$. In order to keep our computations simple we shall use short-range potentials of the type

$$V_{sl} = - \sum_{i=1}^N |g_{l,\beta_i}\rangle \lambda_{li} \langle g_{l,\beta_i}|. \quad (2.6)$$

Moreover, we take form factors $\langle pl | g_{l,\beta} \rangle$ which are simple rational functions of p ,

$$\langle pl | g_{l,\beta} \rangle = \left[\frac{2}{\pi} \right]^{1/2} \frac{p^l}{(p^2 + \beta^2)^{l+1}}. \quad (2.7)$$

Here β plays the role of an inverse-range parameter. The T operator $T_{csl}(k^2)$ corresponding to the separable potential V_{sl} is separable, too, and may be written

$$T_{csl} = - \sum_{i,j=1}^N |g_{l,\beta_i}^c\rangle (\tau_l^c)_{ij} \langle g_{l,\beta_j}^c|. \quad (2.8)$$

Here the $N \times N$ matrix τ_i^c is defined via its inverse,

$$((\tau_i^c)^{-1})_{ij} = (\Lambda_l^{-1})_{ij} + \langle g_{l,\beta_i} | G_{cl}(k^2) | g_{l,\beta_j} \rangle, \quad (2.9)$$

with G_{cl} the p.w. Coulomb resolvent, and Λ_l a diagonal matrix of strength parameters with elements $\lambda_{ii}\delta_{ij}$. The superscript c labeling the form factors indicates Coulomb-modified form factors

$$\langle pl | g_{l,\beta}^c(k^2) \rangle = \langle pl | [1 + T_{cl}(k^2)G_{0l}(k^2)] | g_{l,\beta} \rangle, \quad (2.10)$$

with G_{0l} the p.w. free resolvent.

In order to obtain the physical on-shell T matrix we merely need to sandwich the operator $T = T_c + T_{cs}$ between the bra $\langle \vec{k}_\infty - |$ and the ket $| \vec{k}_\infty \rangle$. To obtain the physical half-shell T matrix we need to sandwich T between $\langle \vec{p} |$ and $| \vec{k}_\infty \rangle$. The results for the Coulomb part T_c of T are already given in Eqs. (2.3) and (2.4). The results for the remainder part T_{cs} follow easily from Eqs. (2.8) and (2.9). Obviously we need to know the forms $\langle g_{l,\beta}^c | kl_\infty \rangle$, $\langle g_{l,\beta}^c | pl \rangle$, and the inproducts occurring on the right-hand side of Eq. (2.9). These forms are known in the literature. First, we have⁴ [with $B \equiv (\beta + ik)/(\beta - ik)$]

$$\langle g_{l,\beta}^c | kl_\infty \rangle = \langle g_{l,\beta} | kl + \rangle_c = [i^{i\gamma}\Gamma(l+1+i\gamma)/l!] B^{-i\gamma} \langle g_{l,\beta} | kl \rangle, \quad (2.11)$$

$$\langle kl_\infty - | g_{l,\beta}^c \rangle = \langle g_{l,\beta}^c | kl_\infty - \rangle^* = \langle g_{l,\beta}^c | kl_\infty \rangle. \quad (2.12)$$

Second, the inproducts

$$\langle g_{l,\alpha} | G_{cl}(k^2) | g_{l,\beta} \rangle$$

have been given in Ref. 4 (and sources quoted there) for $l=0$ and 1. For general l , expressions were given in Ref. 7.

Third, closed expressions for $\langle g_{l,\beta}^c | pl \rangle$ have been given for $l=0$ and 1 in Ref. 4 and sources quoted there, and for general l only recently by van Haeringen.⁸ In fact, in Ref. 8 a number of equivalent forms have been given. We have found it convenient to use⁸

$$\langle pl | g_{l,\beta}^c \rangle = \langle pl | g_{l,\beta} \rangle - \langle kl | g_{l,\beta} \rangle \frac{k}{p} Z_l(a; B),$$

$$Z_l(a; B) = X_l(a; B) + i \text{Im} P_l^{(i\gamma, -i\gamma)}(u) + F_{i\gamma}(Ba) P_l^{(-i\gamma, i\gamma)}(u) - F_{i\gamma}(B/a) P_l^{(i\gamma, -i\gamma)}(u),$$

$$F_{i\gamma}(z) \equiv {}_2F_1(1, i\gamma; 1+i\gamma; z),$$

$$F_{i\gamma}(z) + F_{-i\gamma}(1/z) = 1 + e^{\pi\gamma} C_0^2(-z)^{-i\gamma},$$

$$a \equiv (p - k - i\epsilon)/(p + k + i\epsilon); \quad u = (p^2 + k^2)/(2pk),$$

$$X_l(a; B) - i \text{Im} P_l^{(i\gamma, -i\gamma)}(u) = (-)^{l+1} i\gamma \Gamma(l+1+i\gamma) \sum_{m=0}^l \binom{l+m}{l-m} \frac{(a^2-1)^{-m}}{(l-m)!} \\ \times \left[\frac{1}{\Gamma(m+1+i\gamma)} \sum_{\nu=1}^m \frac{(Ba)^\nu}{\nu+i\gamma} - (Ba)^m \sum_{\mu=0}^{l-m-1} \frac{\mu!}{\Gamma(\mu+m+2+i\gamma)} \left(\frac{Ba}{Ba-1} \right)^{\mu+1} \right] \\ - (-1)^l \{ \text{Idem}, a \rightarrow a^{-1} \},$$

where the $P_l^{(i\gamma, -i\gamma)}$ are Jacobi polynomials.

III. THE $\alpha\alpha$ POTENTIAL

Various forms of the $\alpha\alpha$ potential V have been suggested in the literature; see, for example, the sources quoted in Ref. 3. Usually a form is chosen with free parameters, which are determined from a fit to phenomenological phase shifts or experimental cross-section data. In this paper we shall use the $\alpha\alpha$

potential constructed by Rahman *et al.*⁹ Because of the identity of the α particles only even partial waves need to be considered. The Coulomb part of the potential is given by $V_c(r) = 2k\gamma/r$, with $2k\gamma = 0.2758 \text{ fm}^{-1}$. The remaining, short range, part V_s is separable and of the form given by Eqs. (2.6) and (2.7). It is of rank 2 for $l=0$, with an attractive and a repulsive component. The strong

repulsion due to the Pauli exclusion principle obeyed by the nucleons is thus accounted for in a phenomenological way by this potential. For $l=2$ and 4 V_s is of rank 1, and attractive. The potential strength parameters λ_{li} and the inverse-range parameters β_{li} are given in Table I. The values differ slightly from the values given in Ref. 9: We found that the values for $l=2$ given in Ref. 9 gave an inadequate fit to the experimentally determined phase shift δ_2^c .

The Coulomb-modified phase shifts $\delta_l^c(k)$ are given by

$$\cot \delta_l^c - i = -\frac{2}{\pi k} \frac{\exp(2i\sigma_l)}{\langle kl \infty - |T_{csl}(k^2)| kl \infty \rangle}. \quad (3.1)$$

Note that δ_l^c equals the total phase shift δ_l^{tot} minus the pure-Coulomb phase shift σ_l . In Fig. 1 we show the computed phase shifts for $l=0, 2$, and 4 as a function of the energy variable k^2 . Note that δ_0^c changes sign near $E_{\text{lab}}=20$ MeV, in agreement with the experimental data.

IV. RESULTS

In Sec. II we have given all formulas needed to calculate $\sigma_{\text{on}}(x)$ and $\sigma_{\text{half}}(x)$ for the $\alpha\alpha$ potential specified in Sec. III, as a function of $x = \cos\theta$, for various energies. Because of the identity of the α particles, the total scattering amplitudes are given by

$$f_{\alpha\alpha} = f(\cos\theta) + f(\cos(\pi - \theta)).$$

The cross sections are given by $\sigma_{\alpha\alpha} = |f_{\alpha\alpha}|^2$.

In Fig. 2 we give the results for $E_{\text{lab}}=20$ MeV ($k=1 \text{ fm}^{-1}$). We have plotted σ_{on} for the pure Coulomb potential V_c (the curve labeled c), and for $V = V_c + V_s$ with only the $l=0$ projection of V_s taken into account (label 0), with $l=0$ and 2 taken into account (label 2), and with $l=0, 2$, and 4 (label 4). The contribution of the zeroth partial wave is seen to be small. This can be attributed to the fact that δ_0^c has a zero near $E_{\text{lab}}=20$ MeV. Clearly the curves are symmetric with respect to the line $\cos\theta=0$. In the cases of subsequent figures this symmetry holds

TABLE I. Values of the parameters for the $\alpha\alpha$ potential.

l	λ_{li}	β_{li}
0	$\lambda_{01}=2.4 \text{ fm}^{-3}$ $\lambda_{02}=-20 \text{ fm}^{-3}$	$\beta_{01}=0.4 \text{ fm}^{-1}$ $\beta_{02}=1.3 \text{ fm}^{-1}$
2	$\lambda_2=1300 \text{ fm}^{-7}$	$\beta_2=1.5 \text{ fm}^{-1}$
4	$\lambda_4=2.6 \times 10^8 \text{ fm}^{-11}$	$\beta_4=3.0 \text{ fm}^{-1}$

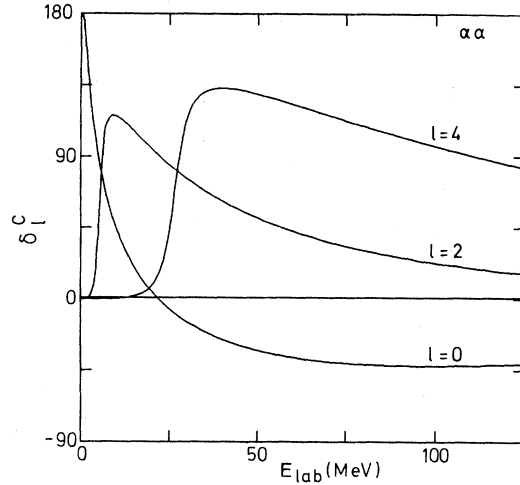


FIG. 1. Phase shifts δ_l^c for $l=0, 2$, and 4, for the potential-parameter values given in Table I, as a function of the energy in the laboratory system, E_{lab} .

too, and henceforth we shall consider only values of $\cos\theta$ between 1 and 0.

For the same energy $E_{\text{lab}}=20$ MeV we have plotted σ_{half} in Fig. 3. The labels 1, 2, 3, and 4 refer to values of the off-shell-momentum variable p , which are "increasingly off-shell": $p/k=1.001, 1.01, 1.1$, and 1.2, respectively. The four cases c ; $c+l=0, c+l=0, 2, c+l=0, 2, 4$ (in an obvious shorthand notation) are given in Figs. 3(a)–(d), respectively.

In the remaining figures we shall display only re-

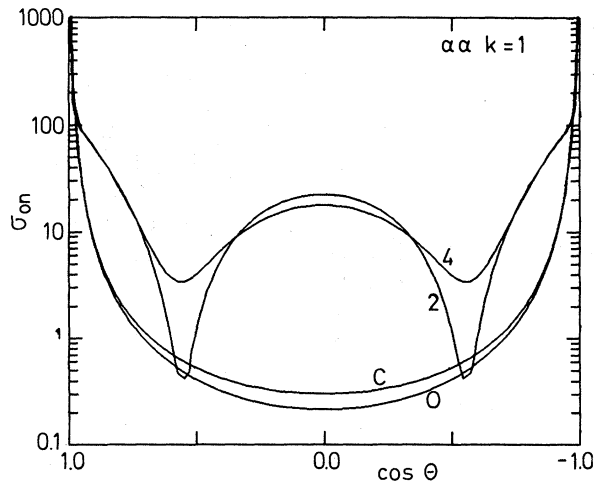


FIG. 2. On-shell cross section σ_{on} for (free) $\alpha\alpha$ scattering for $k=1 \text{ fm}^{-1}$ ($E_{\text{lab}}=20$ MeV) in units fm^2 , plotted versus $\cos\theta$. The curves labeled $c, 0, 2$, and 4 correspond to the pure Coulomb case, and additional inclusion of one, two, or three partial waves in V_s , respectively.

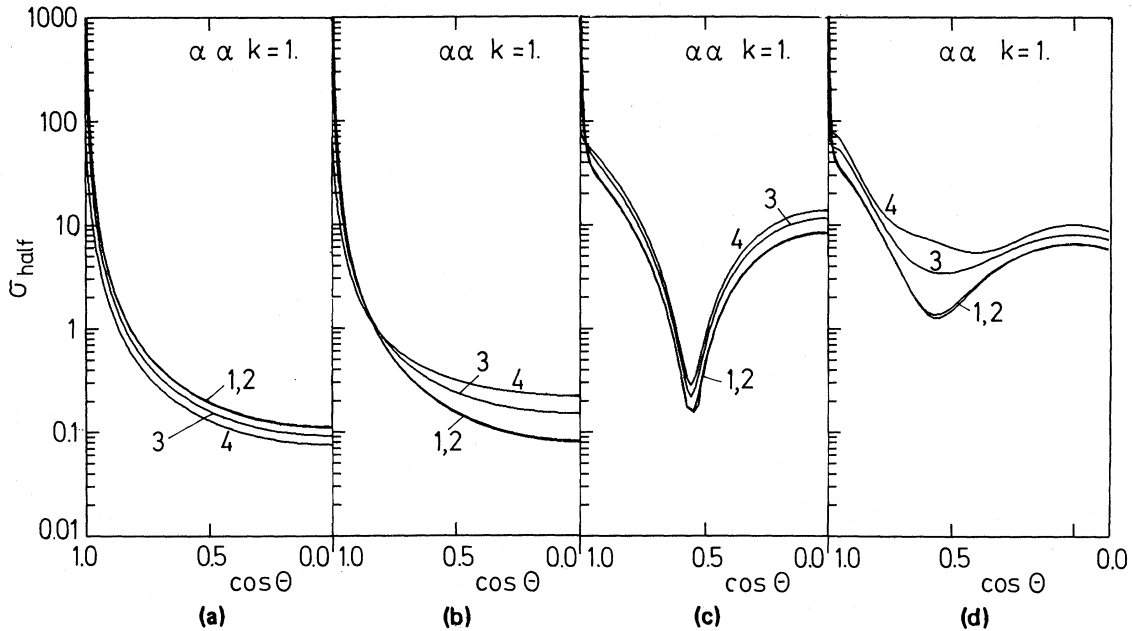


FIG. 3. Half-shell cross section σ_{half} for $\alpha\alpha$ scattering for $k=1 \text{ fm}^{-1}$ ($E_{\text{lab}}=20 \text{ MeV}$) in units fm^2 , plotted versus $\cos\theta$. The labels 1, 2, 3, and 4 in each case indicate the value of the off-shell variable $p/k=1.001, 1.01, 1.1, \text{ and } 1.2$, respectively. (a), (b), (c), and (d) correspond to inclusion of zero, one, two, or three partial waves in V_s , respectively (cf. Fig. 2 and text). $C_0^2=0.3721$.

sults with all three partial waves included in V_s ($l=0, 2, \text{ and } 4$). In Figs. 4(a)–(c) we have plotted σ_{on} , σ_{half} , and their ratio $\sigma_{\text{half}}/\sigma_{\text{on}}$, respectively. The top row corresponds to $E_{\text{lab}}=5 \text{ MeV}$ ($k=0.5 \text{ fm}^{-1}$), the bottom row corresponds to $E_{\text{lab}}=80 \text{ MeV}$ ($k=2 \text{ fm}^{-1}$).

The full lines in Fig. 5 give the ratio $\sigma_{\text{half}}/\sigma_{\text{on}}$ as a function of E_{lab} . Again the labels 1, 2, 3, and 4 designate the off-shell-variable values $p/k=1.001, 1.01, 1.1, \text{ and } 1.2$, respectively. The four cases $\cos\theta=0, 0.25, 0.5, \text{ and } 0.75$ are shown. The broken lines in Fig. 5 show the corresponding results in the case that the Coulomb potential between the α particles is switched off artificially.

V. DISCUSSION

In this paper we have chosen to represent the $\alpha\alpha$ interaction by the potential obtained in a phenomenological way by Rahman *et al.*⁹ It contains the (point-particle) Coulomb potential. In addition it contains a part which is separable of rank 2 for $l=0$, of rank 1 for $l=2$, and also of rank 1 for $l=4$. In order not to obtain an unacceptable fit to the experimental phase shifts we had to change the value of one potential parameter, cf. Ref. 9 and

Table I. We have chosen this potential because with this choice a large part of the computations can be carried out analytically. Clearly the potential is not realistic in the following respects:

(i) The high-energy tail of the phase shifts does not follow the experimental data. For example, for the D wave $\text{Re}\delta_2^0$ experimentally changes sign near $E_{\text{lab}}=110 \text{ MeV}$, while our δ_2^0 remains positive, cf. Fig. 1.

(ii) Above the first inelastic threshold absorptive effects play a role. These can be simulated by considering a complex energy-dependent potential V_s . In this paper, however, we only consider a real V_s .

(iii) At higher energies more partial waves are needed. This is illustrated in Fig. 2, which strongly suggests that the partial-wave sum has not yet reached full convergence. Yet, we feel that our model potential is fully adequate to gain a qualitative understanding of the half-shell scattering process.

In the formalism in Sec. II Coulombian asymptotic states $|\vec{k}_{\infty\pm}\rangle$ and $|kl_{\infty\pm}\rangle$ have been used. The reader who is not familiar with the use of these states is referred to Ref. 10. The use of these states is particularly convenient when working in the momentum representation with separable potentials

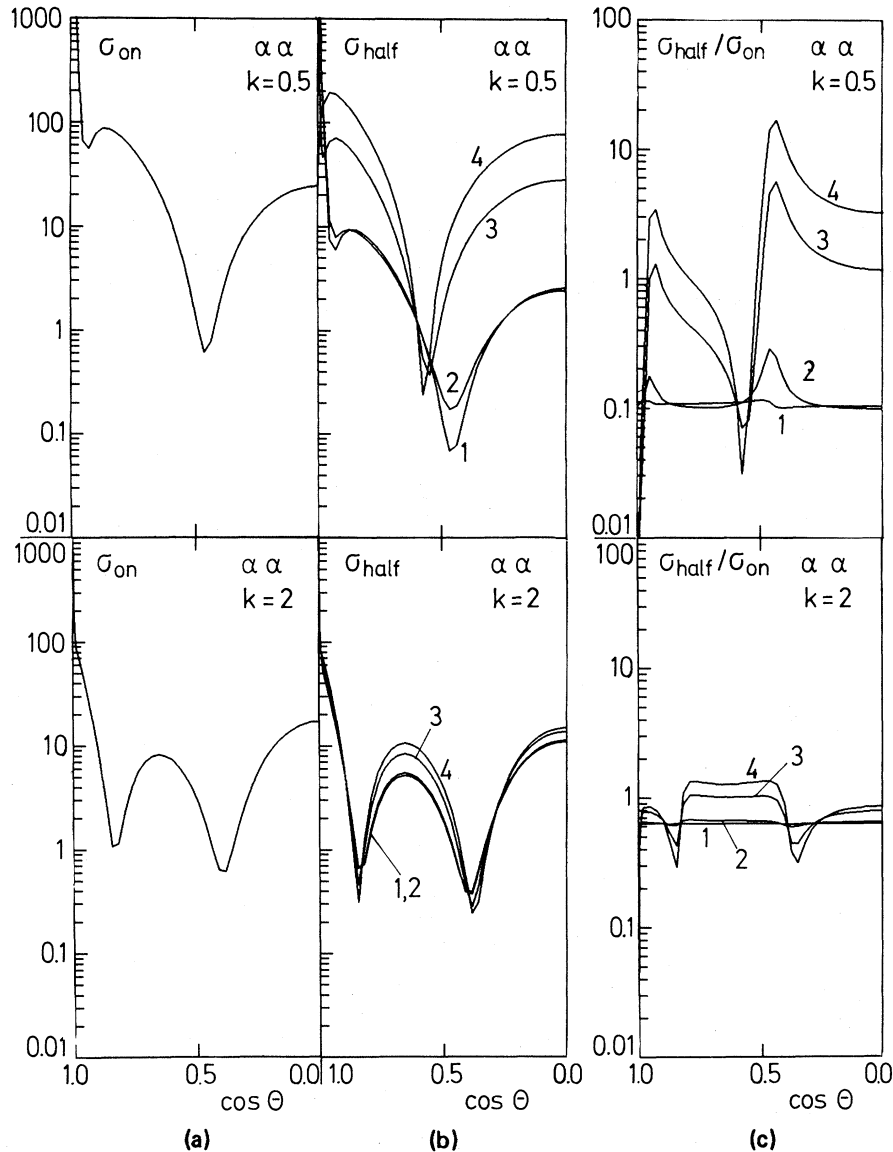


FIG. 4. The upper row corresponds to $k=0.5 \text{ fm}^{-1}$ ($E_{\text{lab}}=5 \text{ MeV}$, $C_0^2=0.1118$). The bottom row corresponds to $k=2 \text{ fm}^{-1}$ ($E_{\text{lab}}=80 \text{ MeV}$, $C_0^2=0.6286$). (a) Plot of σ_{on} in units fm^2 against $\cos \theta$. (b) Plot of σ_{half} against $\cos \theta$, for $p/k=1.001$, 1.01, 1.1, and 1.2, respectively, labeled 1–4 in this order. (c) Plot of the ratio $\sigma_{\text{half}}/\sigma_{\text{on}}$. The meaning of the labels is the same as in (b).

V_s . Alternatively (at the cost of much numerical work) one can use a procedure of screening the Coulomb potential by an exponential factor $\exp(-r/R)$, with R very large compared to the typical length parameters in V_s . In Ref. 11 we have provided evidence in the pure Coulomb case that such an (un)screening procedure (where for each finite value of R one works with the familiar short-range formalism) leads to a discontinuity⁶ of σ_{half} considered as a function of the half-shell variable p in

the on-shell point $p=k$. This discontinuity is clearly expressed by Eq. (2.5). In fact, it is not difficult to show from the explicit formulas at the end of Sec. II the presence of this discontinuity for the case of our $\alpha\alpha$ potential.

In a previous attempt¹² to describe half-shell scattering of charged particles (the pp system), this discontinuity did not receive the attention that it deserves. Some other observations in Ref. 12, dating back to 1972, need careful reconsideration.

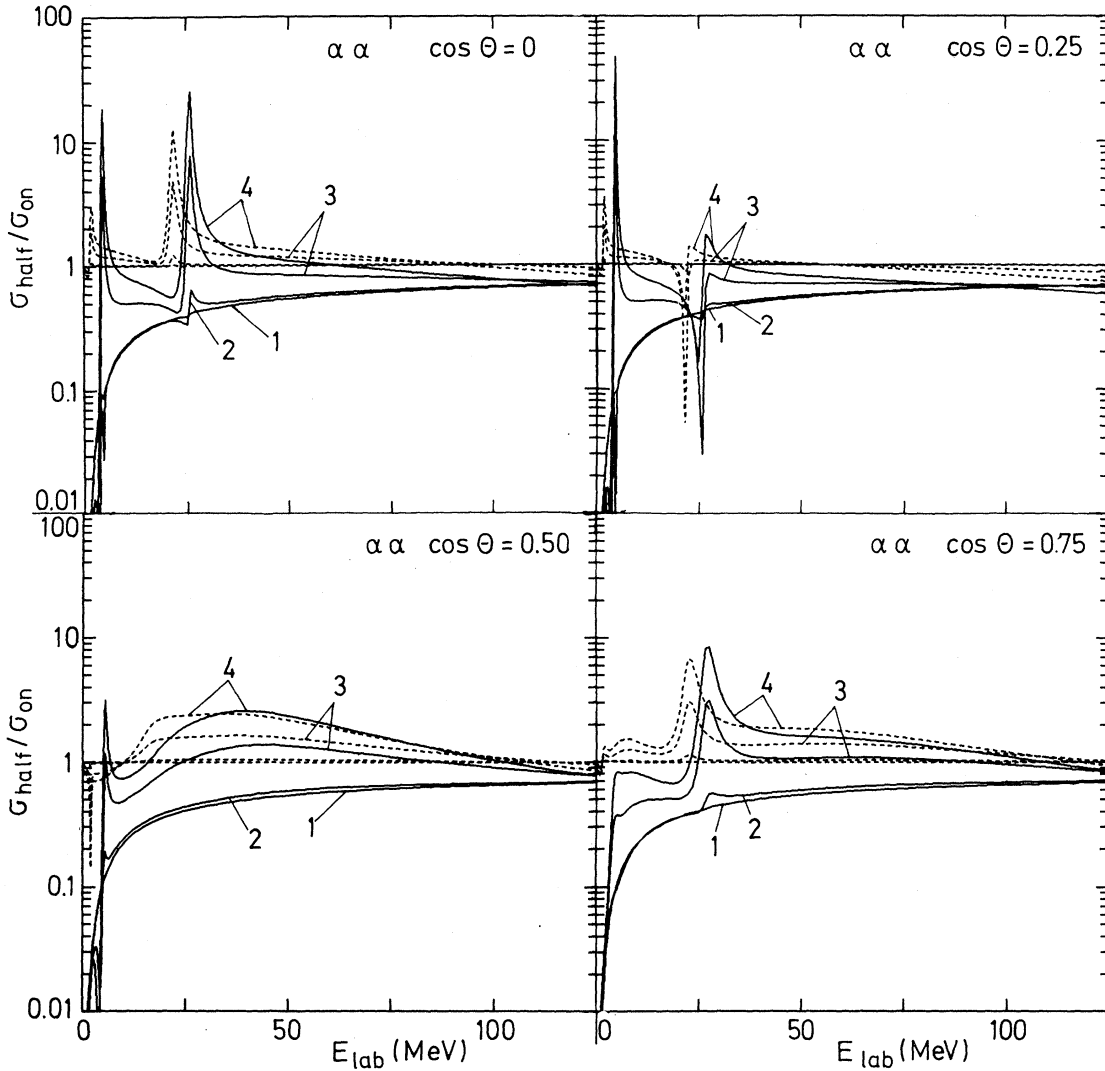


FIG. 5. Full lines: plots of $\sigma_{\text{half}}/\sigma_{\text{on}}$ vs E_{lab} for the full $\alpha\alpha$ interaction V . The labels 1–4 have the same meaning as in Figs. 3 and 4. The four different plots correspond to $\cos\theta=0, \frac{1}{4}, \frac{1}{2},$ and $\frac{3}{4}$, respectively. Broken lines: the same, but now the Coulomb interaction in $V=V_c+V_s$ has been switched off (i.e., $V=V_s$).

We point out that f_{on} and f_{on}^c [cf. Eqs. (2.1) and (2.3)] are nonintegrable with respect to $\hat{k}\cdot\hat{k}'$ in the forward direction. The same holds for their Born approximations, which are essentially given by $\langle \vec{k}' | V | \vec{k} \rangle$ and $\langle \vec{k}' | V_c | \vec{k} \rangle$, respectively, with $k'=k$. Connected with this is the divergence of the (Coulomb) p.w. series. This problem was solved by Taylor¹³ by the introduction of suitable test functions. The problem of nonintegrability does not exist for the physical half-shell T matrices [cf. Eqs. (2.2) and (2.4)]. These objects, and their Born approximations $\langle \vec{p} | V | \vec{k} \rangle$ and $\langle \vec{p} | V_c | \vec{k} \rangle$, $p \neq k$, are integrable with respect to $\hat{p}\cdot\hat{k}$, and have convergent

p.w. series. Similar remarks apply to the fully off-shell T -matrix elements

$$\begin{aligned} &\langle \vec{p}' | T(k^2) | \vec{p} \rangle, \\ &\langle \vec{p}' | T_c(k^2) | \vec{p} \rangle, \end{aligned}$$

and their Born approximations $\langle \vec{p}' | V | \vec{p} \rangle$ and $\langle \vec{p}' | V_c | \vec{p} \rangle$, with $p' \neq k \neq p \neq p'$.

Let us discuss the results for σ_{half} , displayed in Figs. 3–5. In the DWIA the half-shell-momentum variable p generally is larger than the on-shell value k . We therefore have given only results for $p > k$. In case p is very close to k (e.g., all curves labeled 1,

indicating $p/k=1.001$) σ_{half} is virtually equal to $C_0^2 \times \sigma_{\text{on}}$. This means that (i) considered as a function of $\cos\theta$, the curves for σ_{half} have virtually the same behavior as σ_{on} ; an exception is the extreme forward direction where σ_{on} diverges, whereas σ_{half} does not; (ii) their normalization is different by an energy-dependent factor C_0^2 ; and hence (iii) for low energies especially, the normalization is affected very much.

It should be stressed that the free $\alpha\alpha$ cross section varies quite rapidly with energy and scattering angle, often by orders of magnitude.¹⁴ For all other values of p/k which we considered (curves 2, 3, and 4) we observe that the gross structure of the angular dependence of σ_{half} remains the same and only minima are shifted or filled to some extent, compared to those of σ_{on} . This can lead to a rather wild angular dependence of $\sigma_{\text{half}}/\sigma_{\text{on}}$, however, as is clearly seen in Fig. 4(c). In particular the curves labeled 4 (i.e., $p/k=1.2$) show marked variations in Figs. 4(c) and 5. It should be appreciated that for this case one is already quite far off the energy shell (44%).

In Ref. 15 (cf. also Ref. 1) experimental data for σ_{half} at E_{lab} near 130 MeV are given in the angular range $45^\circ < \theta < 90^\circ$, together with σ_{on} for two neighboring energies. Shape and magnitude of these experimental half-shell and on-shell data agree rather well with each other, if one allows for deviations of the order of 50% in the data which cover more than two decades in magnitude. This is the same order of

deviation which we find between the theoretical curves σ_{half} and σ_{on} at $E_{\text{lab}}=125$ MeV, at most approximately 40% (cf. Fig. 5).

For four $\alpha\alpha$ -potential models Sharma and Jain³ have computed $\sigma_{\text{half}}/\sigma_{\text{on}}$ for various energies and angles. They did not include Coulomb effects rigorously. We support their conclusion that half-shell effects are large (below 140 MeV). They also found that the behavior of the half-shell factor is similar for all the four potentials, one of which is separable. We therefore feel justified in considering only one potential model. We do stress that Coulomb effects are important in the computation of $\sigma_{\text{half}}/\sigma_{\text{on}}$. This importance has been underestimated in Ref. 3, in particular at low energies. Probably this is due to the approximate character of the calculations presented there.

Finally, we wish to point out that in this paper we have merely shown how to compute σ_{half} for $\alpha\alpha$ scattering. We have not discussed the validity of the factorized form in Eq. (1.1), which occurs in the DWIA treatment of $(\alpha, 2\alpha)$ reactions. An investigation of the factorization property in the presence of clusters with relatively large charges (large Sommerfeld parameters) is highly desirable.

One of us (L.P.K.) is happy to acknowledge useful discussions with E. F. Redish and H. van Haeringen, the hospitality of the Theory Group at Maryland, and a Fulbright Travel Grant.

¹H. D. Holmgren, in *Clustering Phenomena in Nuclei*, Proceedings of the International Symposium, Tübingen, 1981, edited by P. Kramer and R. Schultheis (Attempo, Tübingen, 1981), p. 46.

²E. F. Redish, Phys. Lett. **31**, 617 (1973).

³N. R. Sharma and B. K. Jain, Nucl. Phys. **A377**, 201 (1982).

⁴H. van Haeringen, J. Math. Phys. **17**, 995 (1976); **18**, 927 (1977); Ph.D. thesis, Free University, Amsterdam, 1978 (unpublished).

⁵H. van Haeringen and L. P. Kok, Groningen University Reports 128–150, 1979 (unpublished).

⁶L. P. Kok and H. van Haeringen, Phys. Rev. Lett. **46**, 1257 (1981).

⁷N. Maleki and J. Macek, Phys. Rev. A **21**, 1403 (1980);

H. van Haeringen and L. P. Kok, Phys. Lett. **82A**, 317 (1981); H. van Haeringen, *ibid.* **86A**, 359 (1981).

⁸H. van Haeringen, J. Math. Phys. (to be published).

⁹M. Rahman, D. Husain, and S. Ali, Phys. Rev. C **10**, 1 (1974).

¹⁰H. van Haeringen and L. P. Kok, Delft University of Technology Report 8007, 1980 (unpublished).

¹¹L. P. Kok, J. W. de Maag, T. R. Bontekoe, and H. van Haeringen, Phys. Rev. C **26**, 819 (1982).

¹²I. E. McCarthy and P. C. Tandy, Aust. J. Phys. **25**, 237 (1972).

¹³J. R. Taylor, Nuovo Cimento **B23**, 313 (1974).

¹⁴H. E. Conzett *et al.*, Phys. Rev. **117**, 1075 (1960); P. Darriulat *et al.*, *ibid.* **137**, B315 (1965).

¹⁵C. Wang *et al.*, Phys. Rev. C **21**, 1705 (1980).